Zernike Phase Contrast Microscope for EUV mask inspection

Yow-Gwo Wang[a, b], Ryan Miyakawa[a], Andy Neureuther[a, b], and Patrick Naulleau[a]
[a]Center for X-ray Optics, Lawrence Berkeley National Laboratory, Berkeley, CA, 94720
[b]Department of EECS, University of California, Berkeley, CA, 94720

ABSTRACT

In this paper, we address a new inspection method which provides in-focus inspection capability and higher defect sensitivity compared with conventional mask inspection methods. In the Zernike phase contrast microscope, an added phase shift to background wave combines with the phase of bump and pit defects to achieve higher contrast at focus. If we use a centralized apodization to half the lens radius to further reduce the intensity of the phase-shifted background wave, the signal strength can be improved up to 6-fold of its original value. Simulation results further show that this apodization for a typical EUV mask power spectral density results in the noise decreasing in absolute level similar to the clear field reference signal. Thus large improvements in signal to noise ratios are possible with the Zernike phase contrast microscope type systems for EUV mask inspection applications.

Keywords: EUV Mask, Zernike Phase Contrast Microscope, Phase Defect, Mask Inspection

1. INTRODUCTION

To achieve high-volume manufacturing for extreme ultraviolet (EUV) lithography, the quality of EUV masks is key priority. Due to its multilayer characteristics, EUV masks have various kinds of defects that affect the pattern and its subsequent processes [1]. Among these defects, phase defects on EUV mask blank become one of the biggest challenges for EUV lithography to achieve defect-free masks [2]. Even though the height is only a few nanometers on the surface and it is almost invisible at focus due to its phase object characteristics, these bump and pit defects are printable defects on the wafer. Therefore it is important to develop an efficient way to detect these defects on the mask blank level with high defect sensitivity.

Zernike phase contrast microscopy has been developed for many years and is one of the most useful methods to observe phase objects [3]. Live cells for example have very little absorption to light. However, they will create optical path difference as light passes through them due to the difference in the refractive index of cells and the environment. All the information about the structure of the cell is recorded by the phase term. By adding an extra phase shift to the background light, we can align the phases of the background and defect light and enhance the signal strength of the sample. This situation can be applied to phase defects on EUV mask blanks, which similarly only changes the optical path of the light that is projected on it.

In this paper, the performance of Zernike phase contrast microscopy for EUV masks inspection on bump and pit defects is characterized. We apply different phase shifts and different orientations to show in-focus inspection and larger signal strength compared with conventional imaging methods. We also apodize the phase-shifted term to show the possibility of further enhancing defect signals and suppressing speckle noise, which improves the overall signal to noise ratio (SNR).

2. BACKGROUND

2.1 Optical principle for phase contrast and apodization

Phase defects do not change the intensity of the incident light. Instead, they create a phase shift due to the optical path difference compared with the background signal. Therefore, as shown in Figure 1(a), the intensity of background signal is almost the same as measured signal, which makes phase defects almost invisible at focus. However, if we can introduce a phase shift in the background light, then the phase difference can be canceled out between the background and the defect light. The information saved in the defect wave will then have constructive (Figure 1(b)) or destructive (Figure 1(c)) interference with the background light. The resulting wave has better contrast which makes it easier to detect.

Extreme Ultraviolet (EUV) Lithography V, edited by Obert R. Wood II, Eric M. Panning, Proc. of SPIE
Vol. 9048, 904810 · © 2014 SPIE · CCC code: 0277-786X/14/$18 · doi: 10.1117/12.2048180

By contrast, conventional microscopy relies on defocus to introduce the extra phase shift and cannot completely cancel out the phase difference. Multiple steps through-focus are required to achieve adequate phase contrast. Apodization is used to further improve defect sensitivity, which reduces the DC intensity on the pupil plane in order to get better contrast. A schematic diagram is shown in Figure 1(d) for the case of phase contrast and apodization. The increased sensitivity achieved through apodization comes at the expense of throughput.

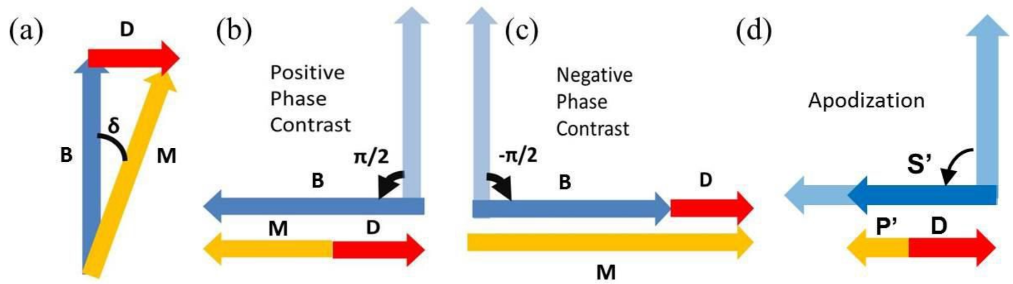

Figure 1. Phasor diagram for phase defect: (a) The conventional situation (0° phase shift). (b) The Zernike phase contrast with 90°phase shift. (c) The Zernike phase contrast with -90° phase shift. (d) The Zernike phase contrast with 90° phase shift and apodization. (B: Background wave, D: Defect wave, M: Measured wave, δ: Original phase shift)

3. SIMULATION RESULTS

3.1 Simulation parameters and settings

Simulation studies using a thin mask scalar imaging model demonstrate the trends in both signal and noise levels. We consider both bump and pit defect with Gaussian profiles, with defect height ranging from 0.5 nm to 1.5 nm and the full width at half maximum (FWHM) from 10 nm to 100 nm. The coherence is defined by disk illumination with a sigma value of 0.5. In order to include phase shift and apodization to improve the defect sensitivity, we modified the pupil function with a ±90° or 180° phase shift which has a shape match to the disk illumination in order to manipulate the background light. Apodization is defined as the transmission of the DC component on the pupil function. Table 1 lists the relevant parameter. In this simulation, we define signal strength as:

$$\text{Signal Strength} = \left| \frac{\text{Peak\_Intensity} - \text{Reference\_ Intensity}}{\text{Reference\_ Intensity}} \right| \quad (1)$$

Table 1. Simulation parameter for Zernike phase contrast microscope on phase defect

Defect Type	**Defect Shape**	**Defect Height (nm)**	**Defect FWHM (nm)**
Bump defect/ Pit defect	Gaussian	0.5~1.5	10~100
NA	**Illumination Type**	**Phase Shift**	**Apodization**
0.2	Disk (0.5 sigma)	±90°, 180°	25%~100%

3.2 Signal strength enhancement and in-focus inspection by the Zernike phase contrast method

Figure 3 shows the aerial images at different defocus levels for both bump and pit defects, with conventional or Zernike phase contrast configurations. The height of the defects are 1 nm and their FWHM are 60 nm. Due to the extra phase shifts added to the background wave, the defect sensitivity has been improved at focus for the phase contrast method, whereas the phase defect is invisible under conventional imaging.

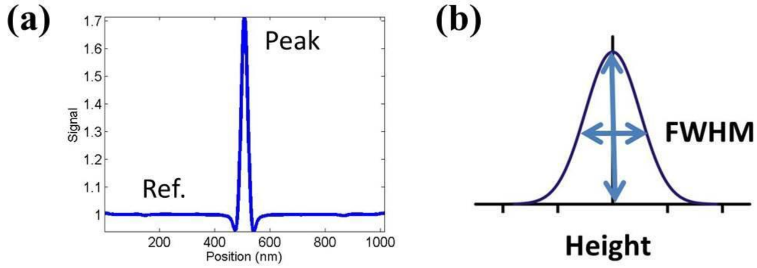

Figure 2. (a) Definition of defect signal strength. (b) Definition of Gaussian shape phase defect

The signal strength at different defocus levels for bump and pit defects utilizing phase contrast vs. conventional methods is shown in Figure 4(a). With the phase contrast method, both bump and pit defects have their peak signal strengths at focus and the signal strength can be improved by 30% at the best situation. This shows the potential to do in-focus inspection for phase defects with an improvement on their defect signals. The differences of the peak signal strength between bump and pit defects are due to the fact that in both cases we apply 90˚ phase shifts to their DC term. This makes the bump defects have constructive interference between the defect wave and the background wave and the pit defects have destructive interference as shown in Figure 4(b).

Since the height of the defect is much smaller than the wavelength of EUV (13.5nm), the phase shift created by the optical path difference is small and thus the 90˚ phase shift can help to cancel out the difference between the background wave and the defect wave. This small angle approximation is only suitable for small defects and the extra phase shift might be different from the 90˚ if the height of the phase object is closer to the wavelength. The lack of a quadrature phase shift will not be able to enhance the signal strength and achieve in-focus inspection of the phase defect. Figure 5 shows the signal strength at different defocus levels with 0˚ (conventional), 90˚, and 180˚phase shifts at pupil function.

3.3 Phase contrast sensitivity to defect height and FWHM

The defect signal will increase as we increase the height of the defect with a fixed FWHM as shown in Figure 6. Interestingly, when defect height is 1.5nm, the signal strength for the bump defect is 1.4 whereas the pit defect is only 0.9. The pit defect signal is not that sensitive when we vary the height. This is due to the fact that it is utilizing a different mechanism to improve the contrast. For pit defects with 90˚ phase shift, the largest destructive interference occurs when the background wave has the same amplitude as the defect wave and both waves cancel. Thus based on our definition, the largest signal strength for destructive interference is 1, which explains why pit defects have lower signal strength than bump defects under a 90˚ phase shift. If we apply a -90˚ instead of +90˚ phase shift to the pupil function, bump defects will utilize destructive interference to improve the defect signal and it will be the bump defects that have lower sensitivity to defect height. Pit defects, which utilize constructive interference to enhance their signal strength, will have larger signal strength than bump defects and better sensitivity to the defect height. The orientation of the phase shift will decide the sensitivity of defect signal to defect height.

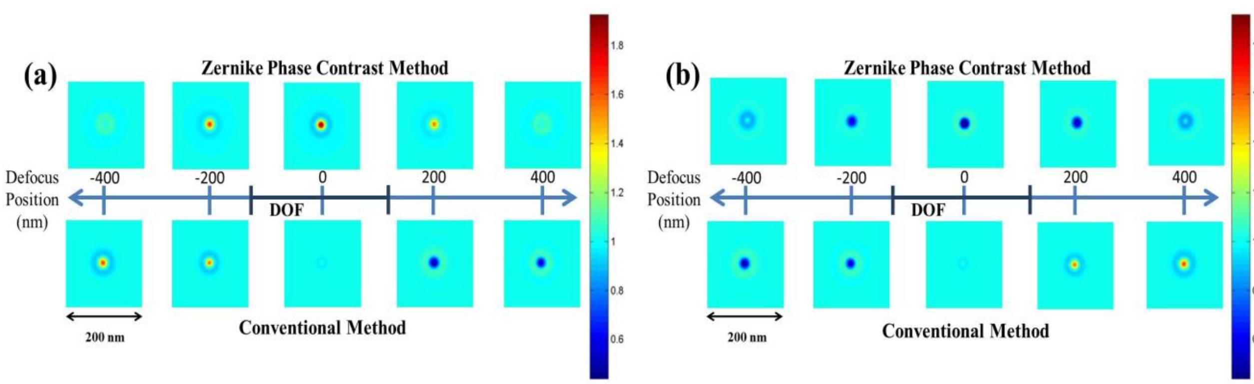

Figure 3. Aerial image for phase defect at different defocus levels with the Zernike phase contrast method (90˚ phase shift) and the conventional method: (a) Bump defect (Height: 1 nm, FWHM: 60 nm). (b) Pit defect (Height: 1 nm, FWHM: 60 nm).

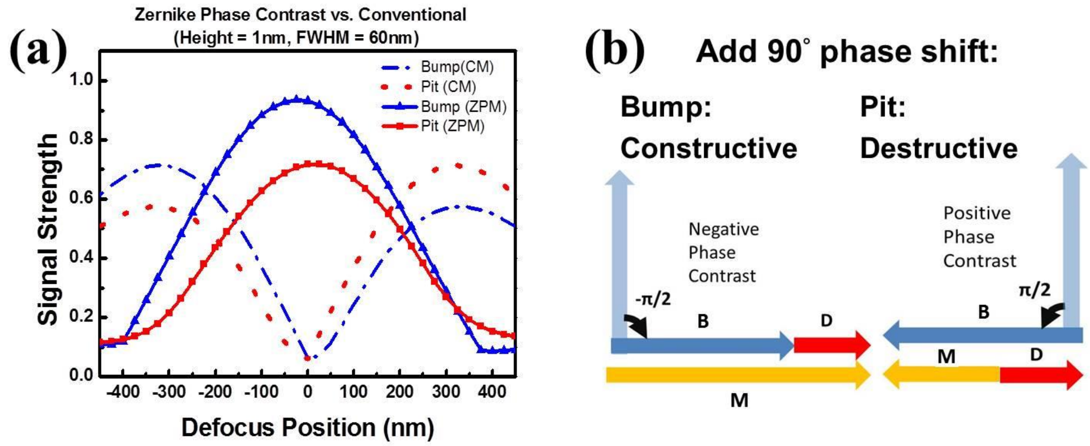

Figure 4. (a) Defect signal strength at different defocus levels for the Zernike phase contrast method (real curve) and the conventional method (dash curve). (b) Phasor diagram for bump defect and pit defect with 90˚ phase shift to its background wave.

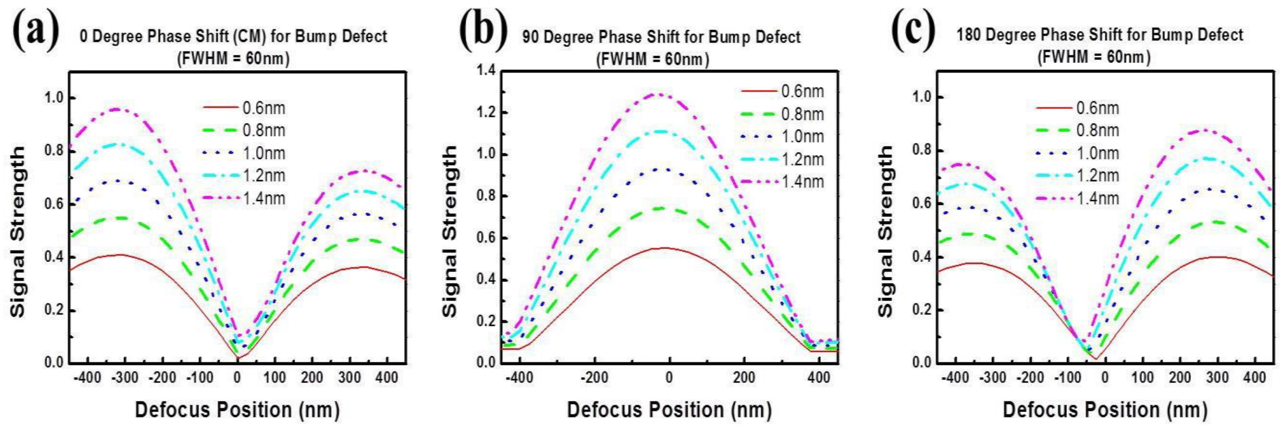

Figure 5. Defect signal strength at different defocus levels for the Zernike phase contrast method with different phase shift: (a) 0˚, (b) 90˚, and (c) 180˚.

If we vary the FWHM of the defect, the position of the peak signal strength will change for the conventional method, but it is not the case for the Zernike phase contrast microscope as shown in Figure 7. This shows another advantage of the Zernike phase contrast microscope; we can collect the largest signal at focus without any dependencies on size and shape. Moreover, the peak signal strength at different FWHM will increase first then decrease when we increase the FWHM of the defect. This can be explained by Figure 8 below. At first stage, below the resolution limit, scattered light from the defect cannot be collected by the pupil due to its large diffraction angle. As we increase the size of the defect, the diffraction angle will become smaller and more light will be collected by the pupil. Thus the signal strength increases. At the second stage, the diffraction angle will decrease as the defect size increases. Part of the diffracted light will get into the central phase-shifted region which is used to phase shift the background wave. Thus the phase contrast effect is reduced and the signal strength will reduce. This indicates that if we want to study defects with different sizes and shapes, an optimized pupil function is necessary in order to gather the defect signal with an acceptable intensity.

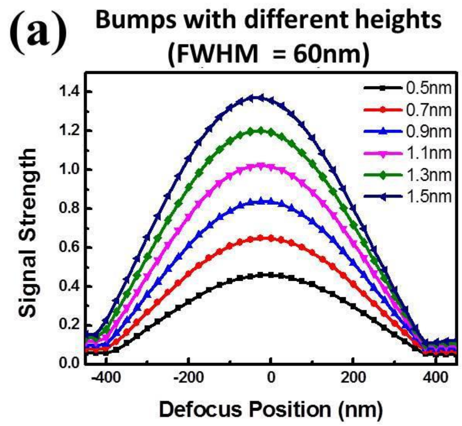

Figure 6. Signal strength of (a) bump defects and (b) pit defects with different heights at different defocus levels.

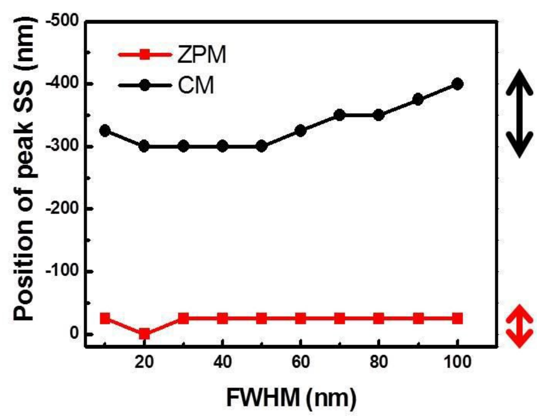

Figure 7. Position of peak signal strength for bump and pit defects with different FWHM (Height: 1 nm) by the conventional method (black) and the Zernike phase contrast method (red).

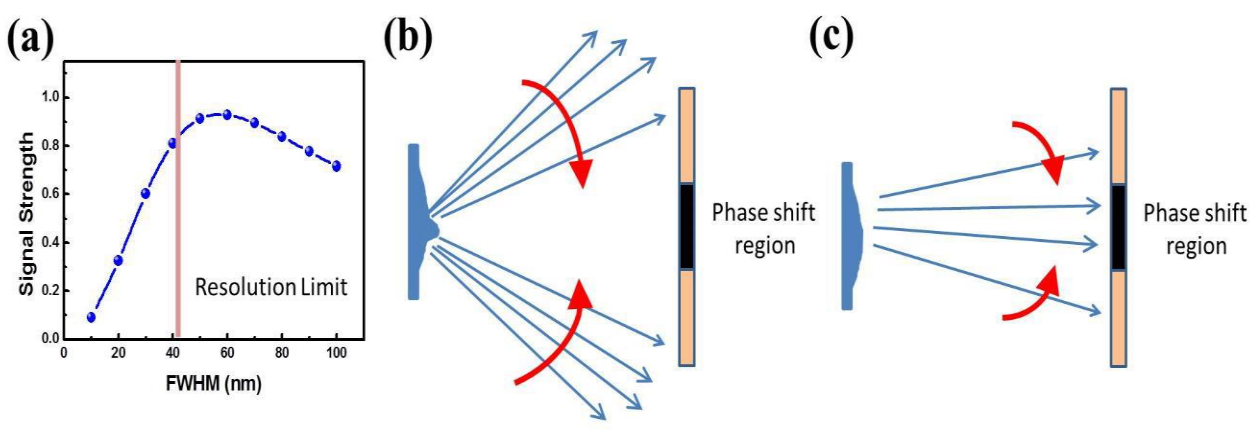

Figure 8. (a)Peak signal strength of bump defects with different FWHM (Height: 1 nm). (b) Schematic diagram of first stage. (Below resolution limit) (c) Schematic diagram of second stage. (Above resolution limit)

3.4 Improvement on signal strength by phase contrast and apodization method

To further improve contrast, we can utilize apodization to reduce the intensity of the background wave to improve defect sensitivity. Figure 9 shows the result for a bump defect with different level of apodization. For the extreme case with only 25% transmission (0.25APD) for the background light, the signal strength has a 500% enhancement compare with the case where we only apply phase shift to the pupil function. As we increase the height of the defect, the signal strength will increase with phase contrast and apodization.

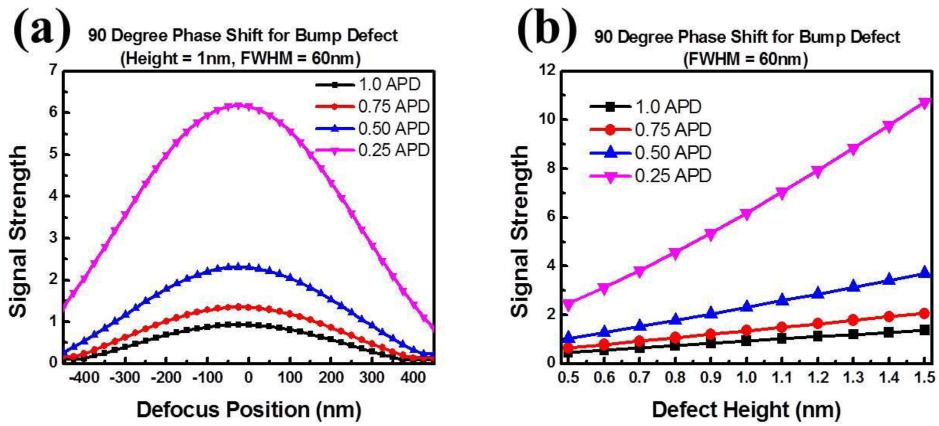

Figure 9. (a)Signal strength of a bump defect (Height: 1 nm, FWHM: 60 nm) with phase contrast and different apodization. (b) Signal strength of bump defects with different heights with phase contrast and different apodization.

3.5 Signal to noise ratio (SNR) enhancement by the Zernike phase contrast microscope with apodization

Ultimately, in enhancing the contrast of phase defects, we are concerned with signal to noise ratio. Therefore, we must also consider the effect of speckle noise from phase roughness. We define signal to noise ratio (SNR) as:

$$\mathrm{SNR} = \frac{\mathrm{Defect\_Signal}}{\mathrm{Speckle\_Noise} + \mathrm{System\_Noise}} \quad (2)$$

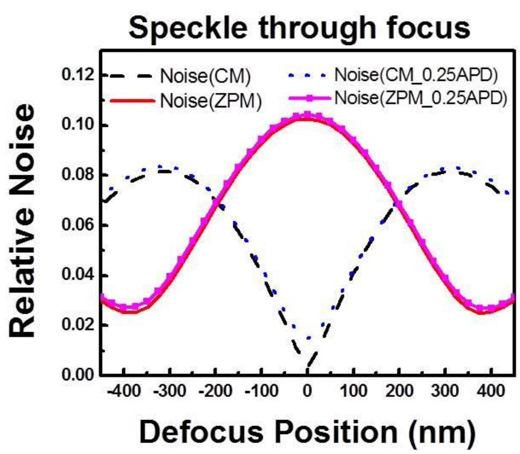

Figure 10. Speckle through focus for the conventional method (black dash), the conventional method with 25 % transmission (blue dot), the Zernike phase contrast method (red), and the Zernike phase contrast method with 25 % transmission (pink square). (Phase roughness: 100 pm.)

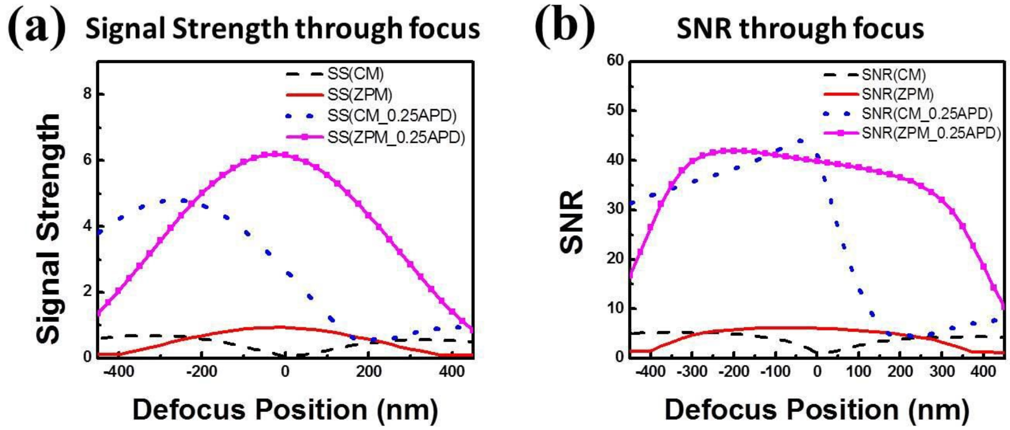

Figure 11. (a)Signal strength of a bump defect at different defocus levels for the conventional method (black dash), the conventional method with 25 % transmission (blue dot), the Zernike phase contrast method (red), and the Zernike phase contrast method with 25 % transmission (pink square). (Height: 1 nm. FWHM: 60 nm.) (b) SNR of a bump defect at different defocus levels for the conventional method (black dash), the conventional method with 25 % transmission (blue dot), the Zernike phase contrast method (red), and the Zernike phase contrast method with 25 % transmission (pink square). (Height: 1 nm. FWHM: 60 nm. Phase roughness: 100 pm. System noise: 5 %.)

To simplify the situation, we limit the system noise to noise not related to the light source. If we consider the apodization, we have to normalize the noise based on different background intensity in order to make the comparison. Thus we define relative noise as:

$$\text{Relative Noise} = \frac{\text{Speckle\_Noise}}{\text{Reference\_ Intensity}} \tag{3}$$

Figure 10 shows the relative noise with four different situations: conventional method (black dash), conventional with apodization (blue dot), phase contrast (red), and phase contrast with apodization (pink square). As expected, the speckle noise will be enhanced by the phase contrast effect. Phase roughness takes the form of phase defects with smaller heights and varying widths. This roughness will follow the same mechanism that phase defects do and get the amplification from the phase contrast effect. However, as shown in Figure 10, the relative noise (normalized to the clear field background) with only apodization (blue dot) is the same as the conventional method (black dash), which means that absolute level of speckle noise is smaller with apodization. This can be explained by the effect shown in the previous section. The difference between phase roughness and phase defects is that the phase roughness has a spectrum of different sizes (FWHM). Thus for those with small lateral size, noise cannot be fully collected by the pupil function. On the other hand, for those with larger lateral size, they will act just like scattered light from buried defects. Noise will get into the reduced transmission region on the pupil and get attenuated. If we relate the phase roughness to the power spectral density (PSD) of phase roughness of the mask, apodization improves SNR by selectively attenuating the many low frequency components of the PSD that only scatter the incident illumination at small angles that remain within the central attenuated region on the pupil. Therefore, the maximum improvement in SNR will depend on the shape of the PSD of the mask roughness if the energy at low frequencies is high. The nearly constant relative noise for both inspection methods in Figure 10 clearly indicates that the absolute level of the noise is being reduced almost exactly the same as the background signal level when apodization is introduced.

The signal strength of a bump defect with different methods is shown in Figure 11(a). Both apodization and phase contrast will increase the defect signal. Thus when we calculate SNR with 5% system noise in Figure 11(b), SNR improvement is mostly due to apodization attenuating the low frequency part of the PSD. Other sources of noise that do not scale with the reference clear field signal may reduce this benefit. This includes stray light that may be proportional to the illumination and detector noise that may be constant at an absolute level.

4. CONCLUSION

In this paper, we demonstrated that with the Zernike phase contrast microscope, in-focus inspection of phase defects can be achieved with a 30% enhancement on signal strength. We also show the phase contrast method gives a fixed position of peak signal strength which is independent of defect size or shape. This provides a promising way to gather defect information at focus. Apodization can further help us to improve the contrast and filter the low frequency components from phase roughness to improve SNR. Therefore, with phase contrast and apodization, a faster and more convenient method can be achieved for EUV mask phase defect inspection. To implement these features at EUV, one could, for example, use a Ru or Mo thin film to achieve the 90° phase shift and apodization. For example, a 30 nm thick Ru film introduces 90° phase shift with 60% transmission. This will increase bump defect signal strength to 240% of its original value over the conventional method (Height: 1 nm, FWHM: 60 nm). More importantly, this signal strength can be detected at focus, and the absorption of Ru can further attenuate the speckle noise to improve the SNR of the inspection system. The other way to incorporate this functionality is by using a Fresnel zone plate. Zone plates can be designed to include phase shifting and apodization [4] for Zernike phase contrast microscopy in EUV and x-ray regimes [5]. We plan on testing this method at EUV in the SEMATECH zoneplate mask inspection microscope (SHARP) at LBNL. Table 2 sums up the performance comparison between the conventional and the Zernike phase contrast microscopes.

Table 2. Comparison between phase contrast, apodization, phase contrast with apodization and conventional method

	Conventional Microscope	**Conventional Apodization Microscope**	**Phase Contrast Microscope**	**Phase Contrast Apodization Microscope**
Scan Mode	Through-focus	Through-focus	In-focus	In-focus
Position of Peak Signal Strength	Varied	Varied	Fixed	Fixed
Signal Strength	100%	680%	134%	867%
SNR	100%	782%	115%	762%
Throughput	100%	25%	100%	25%

ACKNOWLEDGEMENT

This research is sponsored by IMPACT+ (Integrated Modeling Process and Computation for Technology). Member companies – Applied Materials, ARM, ASML, Global Foundries, IBM, Intel, KLA-Tencor, Marvell Technology, Mentor Graphics, Panoramic Tech, Photronics, Qualcomm, Samsung, SanDisk and Tokyo Electron.

This work was performed in part at Lawrence Berkeley National Laboratory which is operated under the auspices of the Director, Office of Science, of the U.S. Department of Energy under Contract No. DE-AC02-05CH11231.

REFERENCES

[1] Kamo, T., Terasawa, T., Yamane, T., Shigemura, H., Takagi, N., Amano, T., Tanaka, T., Tawarayama, K., Suga, O., Mori, I., "Printability of EUVL mask defect detected by actinic blank inspection tool and 199-nm pattern inspection tool", Proc. SPIE 7823, 78231U (2010).

[2] Huh, S., Ren, L., Chan, D., Wurm, S., Goldberg, K., Mochi, I., Nakajima, T., Kishimoto, M., Ahn, B., Kang, I., Park, J., Cho, K., Han, S., Laursen, T., "A study of defects on EUV masks using blank inspection, patterned mask inspection, and wafer inspection", Proc. SPIE 7636, 76360K (2010).

[3] Zernike, F., "How I discover phase contrast," Science 121, 345-349 (1955).

[4] Cheng, G., Hu, C., Xu, P., Xing, T., "Zernike apodized photon sieves for high-resolution phase-contrast x-ray microscopy," Opt. Lett. 35, 3610-3612 (2010).

[5] Youn, H., Jung, S., "Hard X-ray microscopy with Zernike phase contrast," J. Microsc. 223, 53-56 (2006).